A Quantitative Tri-fluorescent Yeast Two-hybrid System: From Flow Cytometry to *In cellula* Affinities

Authors

David Cluet, Ikram Amri, Blandine Vergier, Jérémie Léault, Astrid Audibert, Clémence Grosjean, Dylan Calabrési, and Martin Spichty

Correspondence

martin.spichty@ens-lyon.fr

Graphical Abstract

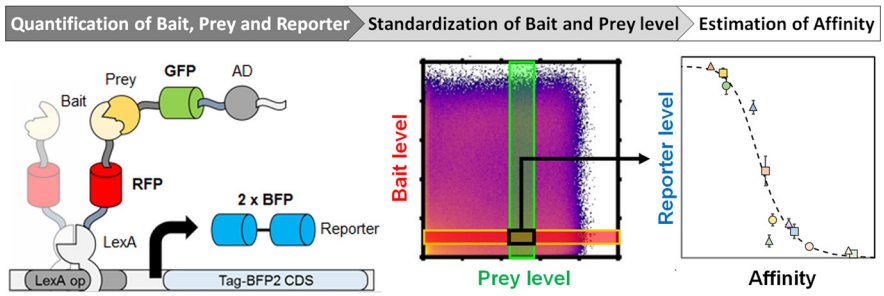

In Brief

We present a novel quantitative yeast two-hybrid (qY2H) system based on fluorescent fusion proteins. It permits simultaneous quantification of Bait, Prey and reporter levels by flow cytometry. We validate the applicability of this qY2H system on a small but diverse set of PPIs with dissociation constants ranging from 117 pM to 17 μM. With our qY2H assay it is straightforward to construct an affinity ladder that permits rapid classification of PPIs with thus far unknown affinities.

Highlights

- Simultaneous quantification of Bait, Prey and Reporter at the single cell level.
- Two hours of reaction are enough instead of 24–48 h for conventional assays.
- Potential expression problems of the Bait and Prey can be easily detected.
- True positive PPIs feature a distinct pattern of Reporter level *versus* Bait/Prey level.
- PPIs with unknown affinities can be ranked using an affinity ladder.

Cluet et al., 2020, Molecular & Cellular Proteomics *19*, 701–715
April 2020 **© 2020 Cluet et al. Published under exclusive license by The American Society for Biochemistry and Molecular Biology, Inc.**
https://doi.org/10.1074/mcp.TIR119.001692

A Quantitative Tri-fluorescent Yeast Two-hybrid System: From Flow Cytometry to *In cellula* Affinities*[S]

David Cluet, Ikram Amri, Blandine Vergier, Jérémie Léault, Astrid Audibert, Clémence Grosjean, Dylan Calabrési, and Martin Spichty‡

We present a technological advancement for the estimation of the affinities of Protein-Protein Interactions (PPIs) in living cells. A novel set of vectors is introduced that enables a quantitative yeast two-hybrid system based on fluorescent fusion proteins. The vectors allow simultaneous quantification of the reaction partners (Bait and Prey) and the reporter at the single-cell level by flow cytometry. We validate the applicability of this system on a small but diverse set of PPIs (eleven protein families from six organisms) with different affinities; the dissociation constants range from 117 pM to 17 μM. After only two hours of reaction, expression of the reporter can be detected even for the weakest PPI. Through a simple gating analysis, it is possible to select only cells with identical expression levels of the reaction partners. As a result of this standardization of expression levels, the mean reporter levels directly reflect the affinities of the studied PPIs. With a set of PPIs with known affinities, it is straightforward to construct an affinity ladder that permits rapid classification of PPIs with thus far unknown affinities. Conventional software can be used for this analysis. To permit automated analysis, we provide a graphical user interface for the Python-based FlowCytometryTools package. ***Molecular & Cellular Proteomics 19: 701–715, 2020. DOI: 10.1074/mcp.TIR119.001692.***

Protein-protein interactions (PPIs)[1] are essential for many functions in living cells, including communication of signals, modulation of enzyme activity, active transportation, or stabilization of the cell structure by the cytoskeleton (1–4). Resolving the complex cellular network of PPIs remains one of the major challenges in proteomics (5). Thus, the quest for reliable methods that identify PPIs and quantify their strength is unbroken.

The yeast two-hybrid technique (Y2H) is a commonly used approach to probe the interaction between proteins (6–8). In contrast to biochemical *in vitro* methods (such as mass spectrometry, ITC or SPR) that require purified proteins, Y2H is based on a genetic assay. It relies on the *in cellula* expression of fusions of the two proteins of interest, usually named Bait and Prey. Upon physical interaction of Bait and Prey, a functional transcription factor is reconstituted that drives the expression of a reporter gene (*e.g.* β-galactosidase). Therefore, a read-out is observed (*e.g.* color, fluorescence, or growth) that permits high-throughput screens; see for example Refs (9, 10).

Y2H has been extensively used in the past decades to decipher PPI networks (11, 12). With growing experience, the scientific community became aware of the limitations of this approach. Standard Y2H is prone to false positive/negative results (8). For example, the absence of a detectable read-out may reflect insufficient expression of the Bait and/or Prey. More laborious Western blottings can be performed to verify the expression (13). Furthermore, Y2H provides often only a qualitative result. With X-gal-based Y2H (14), for instance, the measured read-out (color) cannot be assumed to be proportional to the reporter level, *i.e.* β-galactosidase activity, but exceptions exist (15, 16). Also, the extent of β-galactosidase activity does not necessarily reflect the extent of interaction between Bait and Prey (because of varying expression levels of Bait and Prey fusions). Furthermore, steric effects because of the auxiliary domains BD and AD fused to the Bait and Prey, respectively, may influence the accessibility of the binding interface and thereby alter the interaction strength (13).

Several groups tried to overcome the qualitative limitations of the two-hybrid system in yeast and other organisms. Extensive overviews can be found in the literature, for example Ref (8). Many applied methods could rank PPIs according to their affinity using the quantified read-out, examples are included in Refs (10, 13, 15, 17, 18, 19). It should be noted, however, that mainly mutants were compared. Similar expression levels for the Bait and Prey fusions can be assumed for such mutational studies. Comparing proteins from different families often breaks the correlation (13). It speaks to the need of quantifying not only the read-out but the Bait and Prey

From the Laboratoire de Biologie et Modélisation de la Cellule, Ecole Normale Supérieure de Lyon, CNRS, Université Lyon 1, Université de Lyon, 46 allée d'Italie, 69364 Lyon cedex 07, France

Received July 22, 2019, and in revised form, January 31, 2020
Published, MCP Papers in Press, February 3, 2020, DOI 10.1074/mcp.TIR119.001692

© 2020 Cluet et al. Published under exclusive license by The American Society for Biochemistry and Molecular Biology, Inc.

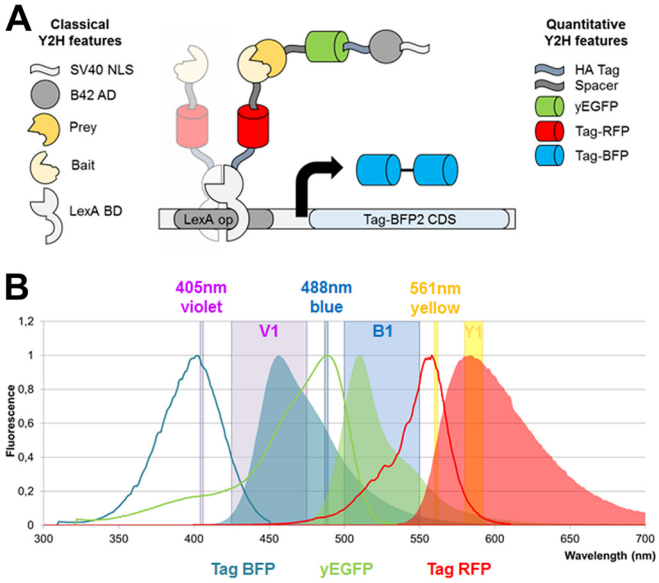

FIG. 1. **Concept of the qY2H approach.** *A*, Our novel Y2H system is based on the one of Brent and coworkers (38). It relies on a split transcription factor where the Bait protein is fused to the LexA DNA-binding domain (BD). The latter binds specifically to the operator of the reporter cassette. The Prey protein is fused to the B42 activation domain (AD). The interaction between BD-Bait and AD-Prey reconstitutes a functional transcription factor that drives the expression of the reporter gene. Our quantitative Y2H approach monitors as a novelty the expression levels of BD-Bait, AD-Prey and the reporter at the single cell level using fluorescent tags. The original fusion proteins when expressed with the constructs of Brent and coworkers are described in the left column of the legend. Our newly added features are presented in the right column. The spacer amino acid sequence is EFGRALE. *B*, The three fluorescent proteins have separated excitation (bold lines) and emission (areas) spectra. Thus, their expression can be easily monitored using compatible flow cytometers. In this work we used a MacsQuant VYB flow cytometer. The three lasers (Violet, Blue, and Yellow) and their respective detection channels (V1, B1, and Y1) are represented as vertical bands.

fusions as well. Thus far, only low-throughput methods exist that address this simultaneous quantification. For example, by measuring the fraction of co-localized fluorescent "Bait" and "Prey" fusions in human cells by high-resolution microscopy (20) it was possible to increase the affinity of an inhibitor (21). Another approach used a fluorescent antibody to quantify the amount of retained Prey by the Bait associated to the periplasm (22). Following this idea, different yeast surface two-hybrid approaches emerged (18, 23) using antibodies or purified proteins.

Here, we present a novel set of Y2H vectors that enable the detection of the reaction partners (Bait and Prey), and the reporter without the need of any antibodies or purified proteins (Fig. 1). Three different fluorescent proteins serve as sensors to probe the cellular expression levels. Thus far, the use of fluorescent proteins in yeast-two hybrid was restricted to either the detection of the Bait or/and Prey proteins (19, 24), or the quantification of the reporter (9, 17, 18, 25). Our quantitative yeast two-hybrid (qY2H) approach permits for the first time the simultaneous quantification of the three proteins at the single cell level by flow cytometry. The new vectors were tested on a set of well-studied protein-protein interactions (26–37). To encompass the sensitivity of the qY2H approach, we selected PPIs that span a wide range of affinities (known from independent *in vitro* experiments), ranging from 117 pM to 17 μM. Finally, we challenged the qY2H system on a set of 59 potential negative controls to test its specificity.

EXPERIMENTAL PROCEDURES

Experimental Design—Starting from the original high copy (2μ) plasmids pLexA and pB42AD (38), several new multiple cloning sites (MCS) were introduced that permit convenient sub-cloning into the expression cassettes via homologous recombination in yeast or Gibson assembly cloning (see supplemental Fig. S1 for detailed vector maps). Thus, the newly designed vectors facilitate the construction of novel fusion proteins with tailored functionalities. Here we generated cassettes that code for BD-Bait, AD-Prey and reporter fusions with several new features as shown in Fig. 1. We copied the HA tag (that was originally only in the AD-Prey expression cassette) to the BD-Bait cassette to enable the simultaneous quantification of expressed BD-Bait and AD-Prey fusions by Western blotting. In addition, we added red and green fluorescent tags (Tag RFP and yEGFP) to the BD-Bait and AD-Prey cassettes, respectively. Furthermore, the original reporter (β-galactosidase) was replaced by a tandem of the Tag-BFP in the 2μ pSH18–34 vector (38). The tandem arrangement of fluorescent proteins is a common strategy to obtain brighter reporters (39, 40). The three fluorescent tags emit at considerably different wavelength ranges so that their individual expression levels can be simultaneously monitored at the single-cell level by flow cytometry (Fig. 1*B*). In addition, a spacer sequence was inserted between the fluorescent tags and the Prey/Bait to reduce potential steric hindrance in the expressed fusions.

To perform the qY2H assay, haploid cells were transformed with either Prey or Bait plasmids; in the latter case we used haploid cells that were previously transformed with the reporter plasmid. Transformed yeast cells were mated and amplified to generate diploid cultures for the desired BD-Bait/AD-Prey couples or controls (see below). Selection and amplification of the diploids occurred in glucose medium which represses the expression of the AD-Prey fusion (under the control of the GAL1 promoter). Transfer of the diploid cells into Galactose/Raffinose medium induced the expression of the AD-Prey fusion and enabled the expression of the reporter.

The reaction was stopped by fixation. The samples were then submitted to flow cytometry measurements (Fig. 2) to monitor the fluorescence intensities at the single cell level for three different channels matching the emission ranges of the fluorescent BD-Bait, AD-Prey and reporter fusions; hereafter these channels are named Tag-RFP-H, yEGFP-H and Tag-BFP-H, respectively.

We analyzed the expression level of the fluorescent proteins either for the entire cell population (to which refer as "global" hereafter) or for subpopulations using interval gatings.

The qY2H approach was validated on the set of PPIs with known *in vitro* affinity given in Table I (Affinity Test Set, ATS). First, the autoactivation potential of each protein was determined when used as Bait or Prey. Therefore, the constructs BD-Bait or AD-Prey were tested in combination with proper controls, *i.e.* AD-Empty and BD-

[1] The abbreviations used are: PPIs, protein-protein interactions; qY2H, quantitative yeast two-hybrid; BD-Bait, DNA binding domain fused to the Bait; AD-Prey, activation domain fused to the Prey; ATS, affinity test set; STS, specificity test set; RRS, random reference set.

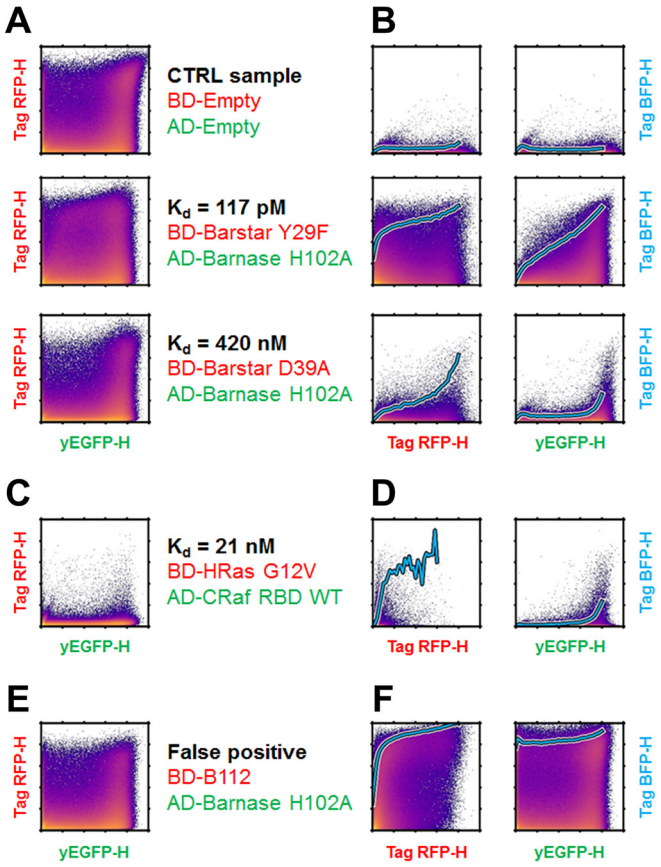

FIG. 2. **Single-cell raw data from the flow-cytometry acquisition.** *A–F,* Fluorescence intensities in the channels corresponding to the BD-Bait (Tag-RFP-H), AD-Prey (yEGFP-H) and reporter (Tag-BFB-H) are represented as density-colored scatter plots for a subset of studied couples. Intensities were pre-processed by a hlog-transformation. The expression of the BD-Bait as a function of AD-Prey is presented in *A*, *C,* and *E*, The expression level of the reporter as function of the BD-Bait or AD-Prey is displayed in *B*, *D,* and *F*, The cyan bold line represents the evolution of the Tag-BFP-H intensity when averaged over the 5% top-ranked cells in slices of the yEGFP-H or Tag-RFP-H channel. In addition to the CTRL sample, a strong (picomolar) and a medium (nanomolar) couple are shown, see *A* and *B*. As an example for low expression, the construct BD-Bait HRas is shown in *C* and *D*. We also constructed a genetic fusion of the LexA BD with the B112 AD as an example of a false positive interaction, see *E* and *F*.

Empty fusions, respectively. The term "Empty" indicates that no coding sequence was fused to the fluorescent BD or AD. If a given BD-Bait fusion protein (paired with AD-Empty) yielded a significantly higher auto-activation than the pair BD-Empty/AD-Empty (named CTRL hereafter), it was not considered suitable for further investigations (see subsection Statistical Analyses of the Experimental Procedures). The same test was carried out for the AD-Prey fusion proteins (paired with BD-Empty).

By exchanging Bait and Prey for a given couple it is possible to probe the corresponding PPI in two different orientations. It is known that the two orientations may lead to different read-outs (13). As a second filter (after the auto-activation filter), we measured therefore for each couple the reporter level for both orientations (see supplemental Fig. S2 and supplemental Data S1). Table I lists the couples in the orientation with the stronger reporter level (when the cellular contents of BD-Bait and AD-Prey are standardized, see below). This orientation is considered as the molecular configuration with the higher accessibility of the PPI binding interface (13). In other words, this orientation may feature the smaller steric hindrance because of the fused fluorescent BD and AD and probably resembles more closely the situation of free (not fused) proteins. We focus therefore in the following sections on the orientation given in Table I.

The entire procedure starting from the transformation up to the flow cytometry measurement was repeated at least three times for each protein-protein interaction with known affinity of Table I.

Often the specificity of Y2H methods is evaluated on a Random Reference Set (RRS) (41, 42). Such sets contain protein pairs unlikely to interact with affinities on the order of those in the ATS. Our qY2H assay was tested on a set of 59 pairs that were obtained by cross-testing a sub-selection of BD-Bait and AD-Prey fusions (from the ATS and from the RRS of RRS of Ref (41)). These fusions were selected based on the following two criteria: (1) avoiding fusions with an auto-activating phenotype, and (2) avoiding fusions with low expression level like BD-HRAS and AD-BLIP. With such weakly expressed fusions, we would risk that there are no cells available for the required analysis (as we have experienced in certain experiments, see for example AD-BLIP in Table II). For some proteins, both criteria are fulfilled when used as BD-Bait and as AD-Prey fusion. In this case, we took the fusion that leads to the higher reporter level when tested in the Affinity Set. For example, Barnase was used as AD-Prey because the couple BD-Barstar/AD-Barnase yields the higher reporter level than BD-Barnase/AD-Barstar. This was done to minimize steric effect issues (see above).

The STS includes the pairs ARMC1/Emerin and GMPPA/MNAT1 from the RRS of Ref (41). These pairs were previously tested with 2μ plasmids in GAL4 Y2H systems (41, 42). The orientation BD-Emerin/AD-ARMC1 yielded a positive signal in three assays out of nine. In the reverse orientation however, the result was negative in all assays (42). The couple BD-MNAT1/AD-GMPPA produced different results depending on the experimental approach (41, 42). We wanted to monitor the behavior of these ambiguous couples in our qY2H system. We tested them in both orientations. In the Specificity Test Set (STS), we included the orientation with the higher reporter level in our qY2H system.

Creation of Plasmids—In order to generate the pSB_1Bait plasmid, the pLexA (38) vector was linearized using EcoRI and SalI (Thermo Scientific) to remove all DNA between the LexA cDNA and the ADH terminator. The Barstar WT coding sequence was ordered for synthesis to Eurofin Genomics as part of a new expression cassette. At the 5′ end we added the sequences of the HA-Tag and our MCS-spacer (EcoRI, *Asc*I, and XhoI). At the 3′ end, after the stop codon of Barstar, we inserted one XhoI site, created 3 stop codons (1 per ORF) and regenerated the *Sal*I site. The upstream (LexA) and downstream (Terminator) 30bp required for homologous recombination in yeasts (43, 44) were also added. This new optimized expression cassette was amplified by PCR (Phusion DNA polymerase, Thermo Scientific, Courtaboeuf, France), using the primers primSB_0001 and 2 (see supplemental Table S1), and inserted in the previously linearized pLexA vector. As a result, we obtained the pSB_1Bait_Barstar. The coding sequence for Tag-RFP was subsequently introduced in the EcoRI site through PCR from pTag_RFP-Actin (Evrogen, Souffelweyersheim, France), using the primers primSB_0003 and 0004, combined with homologous recombination in yeasts to obtain the pSB_1Bait_RFP-Barstar plasmid. The pSB_1Bait_RFP-Empty and pSB_1Bait-Empty vectors were generated by digesting the pSB_1Bait_RFP-Barstar and pSB_1Bait_Barstar, respectively, with XhoI (Thermo Scientific), followed by self-ligation.

To create the pSB_1Prey vector, the pB42AD plasmid (38) was linearized using EcoRI and XhoI. The sequence coding for the non-

toxic Barnase mutant H102A was ordered from Operon MWG (Eurofins Genomics, Ebersberg, Germany). At the 5′ end we inserted the same MCS-spacer sequence as in the pSB_1Bait vector to allow easy transfer from one plasmid to the other. At the 3′ end, we inserted one XhoI site, created 3 stop codons and one NcoI restriction site. The upstream (HA-Tag) and downstream (Terminator) 30bp required for homologous recombination in yeasts were also introduced. This new expression cassette was then amplified by PCR (primSB_0010 and 0011) and inserted in the pB42AD by homologous recombination in yeast to obtain the pSB_1Prey_Barnase-H102A vector. The coding sequence of the yEGFP was amplified from the pGY-LexA-GFP_KanMX (kindly provided by Dr Gaël Yvert) using the primers primSB_0012 and 0013, and then introduced in the EcoRI sit of our MCS as previously to generate the pSB_1Prey_yEGFP-Barnase-H102A vector. The pSB_1Prey-Empty and pB_1Prey_yEGFP-Empty were created by removing the coding sequence of Barnase H102A with XhoI and performing a self-ligation.

The coding sequences of the mutants of Barstar, Ras G12V C186A, TEM, Nef LAI, and CDK2 were ordered to Eurofins Genomics, with extensions for the pSB_1Bait_RFP vector, when those of CRaf RBD WT, CRaf RBD A85K, BLIP1, SRC SH3, and CksHs1 were ordered with extensions for the pSB_1Prey_yEGFP plasmid. The sequences for ARMC1 and Emerin were obtained from a Jurkat cells cDNA library (kindly provided by Dr Emiliano Ricci). All coding sequences were then introduced in the XhoI linearized pSB_1Bait_RFP and pSB_1Prey_yEGFP plasmids using the primers presented in supplemental Table S1. The sequences for Pex3p Q34-K373, Pex3p Q34-K373 W104A, Pex19p (C8A, C128A, C226A, C229A, C296A), MAT1, GMPPA, Grb2 SH3 and Vav1 SH3 were synthetized and cloned into the pSB_1Bait_RFP and pSB_1Prey_yEGFP by Eurofins Genomics. All our constructions were validated by sequencing (GATC Biotech, Eurofins Genomics).

To create the reporter plasmid, the pSH18–34 (38) was digested using the unique SalI (In the modified Gal1 promoter) and *Rsr*II (downstream to the β-Galactosidase coding sequence) restriction sites. We subsequently reconstructed the expression cassette using four PCR products:

1. The Gal1 promoter delta Gal4 with 8 operator LexA and the Kozack sequence with a new downstream MCS (*Asc*I, NheI) (primSB_0076 and 0077).
2. The Gal1 Nterm sequence (I10-C20), originally expressed by the pSH18–34, is used as spacer (primSB-0078 and 0079) between the two copies of the Tag-BFP.
3. The coding sequence of the Tag-BFP (from pTag_BFP-Actin, Evrogen) bordered with 2 XhoI sites, (primSB_0084 and 0085).
4. The terminator sequence (primSB_0080 and 0081).

These 4 amplicons were then used to perform directly a gap repair in yeasts. Thus, we obtained the pSB_3RO plasmid. A second copy of the Tag-BFP (primSB_0120 and 121) was inserted in our new NheI site (Thermo Scientific), by homologous recombination to generate the pBFP2 plasmid. This final vector allows the expression of a dimer of Tag-BFP as reporter of the yeast two hybrid reaction. Final quality control was performed by sequencing (GATC Biotech).

Western Blotting—Total protein extracts were obtained from 6 $OD_{590\ nm}$ exponentially growing diploids yeasts as previously described (45) into 60 μl of sample buffer. Ten microliters were used for SDS-Page analysis on Bolt™ 4–12% Bis-Tris Plus Gels (Thermo Scientific). Electrophoresis separation was performed in NuPAGE™ MOPS SDS Running Buffer (Thermo Scientific). Proteins were then transferred on a Nitrocellulose Membrane 0.45 μm (Bio-Rad), using a Trans-Blot® Turbo™ Transfer System (Bio-Rad, Roanne, France) for 14 min, at 1 A and 25 V. The membrane was subsequently blocked 1 h at room temperature in PBS + tween 0.2% (v/v) supplemented with 5% (w/v) low-fat milk powder. HA tagged proteins were labeled overnight at 4 °C with the mouse HA.11 Clone 16B12 Monoclonal Antibody (Eurogentec, Angers, France) diluted 1/2000 in PBS + tween 0.2% (v/v) + 10 mg/ml BSA (Albumin bovine fraction V, Euromedex, Souffelweyersheim, France). The membrane was then washed four times 7 mins in blocking buffer at room temperature. The membrane was then incubated for one hour at room temperature in presence of a sheep anti-mouse whole IgG HRP (GE Healthcare, Velizy-Villacoublay, France) secondary antibody diluted 1/5000 in blocking buffer. The excess of antibody was removed with two washing steps of 5 mins in PBSt at room temperature. Labeled proteins were then revealed with Super Signal West Pico chemiluminescent substrate (Thermo Scientific) using a Bio-Rad Chemidoc apparatus (Fig. 3), following instructions provided by the suppliers.

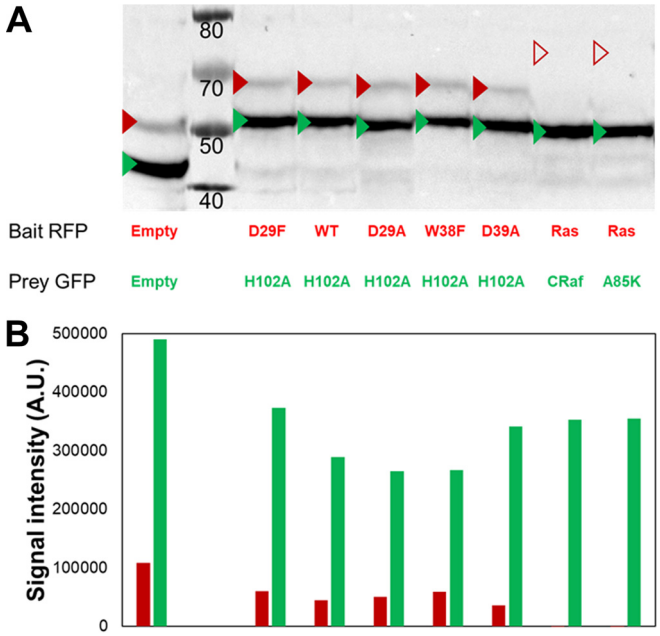

FIG. 3. **Simultaneous detection of BD-Baits and AD-Preys by Western blotting using a single primary antibody.** *A*, The various studied couples were submitted to Western blot analysis. Total proteins were extracted from 6 OD of diploid yeasts grown for 2 h at 30 °C in SGR -UHW (0.25% galactose). The BD-Bait and AD-Prey fusion proteins were simultaneously detected by Western blotting using HA tag (originally present only in the AD-Prey proteins, and newly added to the BD-Bait proteins). The expected molecular weights of the fusion proteins are indicated by red (BD-Bait) or green (BD-Prey) triangles. Except for Ras G12V C186A (empty red triangles), all the proteins are detectable at their correct molecular weight. *B*, The differential expression level was then quantified using ImageJ program. A four to 9-fold overexpression of the AD-Prey compared with the corresponding BD-Bait (when detectable) can be observed.

qY2H in Liquid Phase—Chemo-competent EGY42 (MATa; trp1, his3, ura3, leu2) and TB50 (MATα; trp1, his3, ura3, leu2, rme1) yeasts were generated as previously described (46).

Competent EGY42a yeasts were transformed with 1 μg of pBFP2 and grown on selective S.D.-U medium. Chemo-competent EGY42a pBFP2 yeasts were then generated and transformed with 1 μg of Bait vectors. Haploid Bait yeast strains were then selected on S.D.-UH medium. Competent TB50α yeasts were transformed with 1 μg of Prey vector. Haploid Prey yeast strains were selected on S.D.-W medium. Matrix mating assay were performed for one night with 50 μl of Bait and Prey strains (each) resuspended in YPAD medium at 0.1 OD at 30 °C. The next morning YPAD medium was removed and the

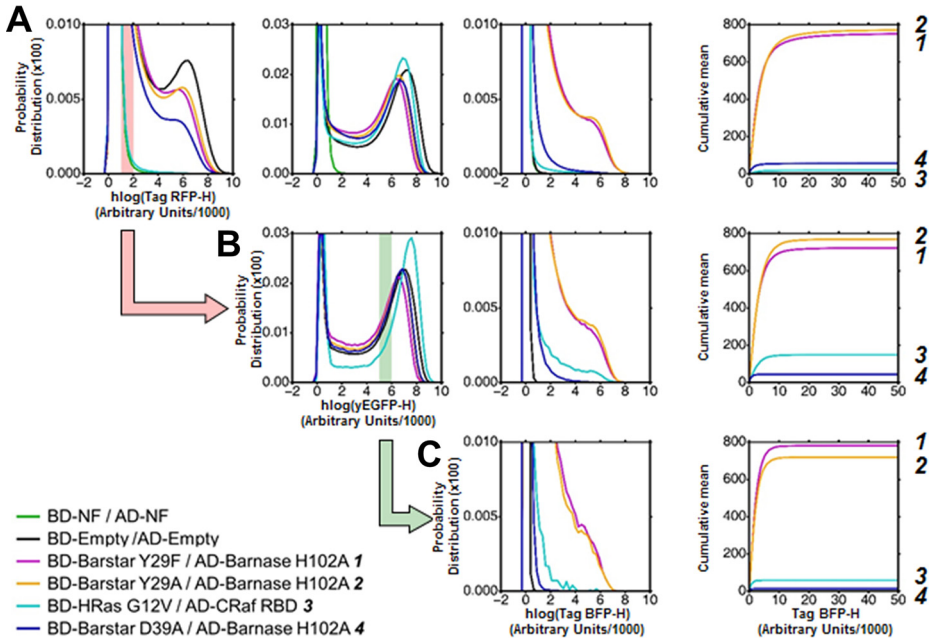

FIG. 4. **Influence of the expression level of BD-Bait and AD-Prey on the reporter level.** *A–C*, The expression levels of BD-Bait (1st column), AD-Prey (2nd) and reporter (3rd) are visualized as a probability distribution of the hlog-transformed fluorescence intensities. In order to better visualize differences in the reporter expression we use an additional representation of the cumulative mean in linear scale (4th column). The distributions and cumulative mean are shown for the global population in *A* and gated subpopulations in *B* and *C*. For reasons of clarity, only an illustrative subset of studied couples is shown. In the legend these couples are ordered and numbered (*1-4*) according to their *in vitro* affinity. The order of the couples according to the reporter expression (*i.e.* mean value of the Tag-BFP-H channel) is given on the very right side of the three subfigures. The global population of cells reveals significant differences in the expression levels of BD-Bait and to a smaller extent of AD-Prey *A*. Because of these expression level differences, the mean values of Tag-BFP-H are ordered differently than the *in vitro* affinities: ***2*** displays a stronger reporter expression than ***1***, and ***4*** stronger than ***3***. Only the discrimination between strong (***1***, ***2***) and medium (***3***, ***4***) interactors is possible. The successive gating of cells, first based on Tag-RFP-H ($700 < \text{Tag-RFP-H} < 900$) values (*B*), and then based on yEGFP-H ($5000 < \text{yEGFP-H} < 6000$) values (*C*), allows to equalize the expression levels. Such standardized subpopulations improve the extraction of quantitative information on the strength of the Bait-Prey interactions: the Tag-BFP-H mean value is ordered according to the *in vitro* affinities. The transparent red bar in the panel of the 1st column shows the Tag-RFP-H gating interval applied to obtain the subpopulation in *B* (symbolized by the red action arrow). Similarly, the green bar and arrow illustrate the yEGFP-H gating interval applied to the subpopulation in *B* to obtain the final subpopulation in *C*.

yeast diploids were harvested and amplified in 1 ml of S.D.-UHW for 3 days at 30 °C.

The qY2H assay was performed in pre-heated (30 °C) and oxygenated SGR-UHW supplemented with Galactose 0.25% (Euromedex) and Raffinose 1% (Sigma-Aldrich, Saint-Quentin-Fallavier, France) to induce the expression of the Prey proteins. To ensure we obtained an excessive number of cells (about 10^7) for the analysis, a culture of 100 ml was inseminated with 600 μl of saturated diploids per couple of interest. It turned out that for a typical analysis 10^6 cells is adequate, so that 10 times smaller cultures and insemination volumes can be used. The yeasts were incubated for 2 h at 30 °C without shaking.

The qY2H reaction was stopped by fixating the yeasts with PFA. Cultures were centrifuged for 10 min at 1000 g, and the yeast were resuspended in 1 ml PBS (Dominique Dutscher, Brumath, France) and transferred into 1.5 ml tubes. After a centrifugation step of 1 min at 13,000 rpm, cells were washed again with 1 ml of PBS. The yeasts were resuspended in 500 μl of PBS 4% PFA (Sigma-Aldrich, Catalog P6148) and incubated for 10 min at 4 °C. The fixation reaction was blocked by 2 washing steps with 1 ml PBS, and one incubation of 15 min at 4 °C in 500 μl of PBS 0.1 M Glycine (Euromedex). Finally, the yeasts were washed twice in PBS, and stored in 1 ml of PBS at 4 °C for not longer than 24 h.

Flow Cytometry—The expression levels of BD-Bait, AD-Prey and reporter were acquired in linear scale using a MacsQuant VYB flow cytometer (the settings are presented in supplemental Table S2), when the lasers reached stable temperature. Calibration beads (Miltenyi Biotech, Bergisch Gladbach, Germany, Catalog 130-093-607) were used prior to all experiments. To ensure homogeneous sampling of the yeasts cells in suspension, we used the strong mixing mode. With the apparatus at our disposal, this mode generates at very early acquisition times a small population of particles with abnormal characteristics for yeast cells (a high red fluorescence intensity, even for non-fluorescent samples). We suspect these are micro-bubbles. To rigorously eliminate this population, we skipped the first 20 000 events of all samples files in the subsequent analysis.

Data Analyses—The flow-cytometry files were analyzed using the FlowCytometryTools package for python (http://eyurtsev.github.io/FlowCytometryTools). For visualization purposes, the hlog-transformation (47) was applied to the signals of the channels TagRFP-H, EGFP-H, TagBFP-H with the following settings: $b = 1000$, $r = 10000$, and $d = 5.4$. The transformed values were then visualized as 2-dimensional scatter plots using the built-in function of FlowCytometryTools (Fig. 2) or as 1-dimensional probability distribution functions (PDFs) using the package matplotlib (Fig. 4). The PDFs correspond to histograms generated with the package NumPy (using 50 bins), normalized so the integral over the range -1000 to 10,000 is 1.

To quantify the reporter level, we calculated the mean value of the Tag-BFP-H channel, $\langle$Tag-BFP-H$\rangle$, either for the entire population

of cells or for double-gated subpopulations. Values of double-gated subpopulations are indicated by double square brackets, [[…]]. If not specified differently, the two gates are: 700 < Tag RFP-H < 900; 5000 < EGFP-H < 6000. The choice of the gates is explained in the section "Recommendations".

To ensure that <Tag-BFP-H> is not dominated by the highest, sparsely sampled Tag-BFP-H values, we checked that the cumulative mean formed a plateau (Fig. 4 and 5). For this purpose, a histogram of Tag-BFP-H values within the range 0–50000 (on a linear scale) was generated using 25 bins. The histogram value of bin i (*i.e.* number of events in bin i) and its lower edge are given by N_i and I_i, respectively. The bins are ordered so that $I_i < I_{i+1}$. With the aid of this histogram, the cumulative mean of the reporter level was plotted with the package matplotlib for increasing values of I_i:

$$\text{Cumulative mean } (I_i) = \frac{1}{N_{tot}} \sum_{j=1}^{i} I_j N_j \qquad \text{(Eq. 1)}$$

where N_{tot} is the total number of events within the data range 0 to 50,00 for the given sample. For $I_i \rightarrow$infinity, the cumulative mean approaches the population mean but it remains slightly smaller because of binning issues. We provide a Python based program with a graphical user interface that automates the calculation of the cumulative mean for large data sets (see section Data Availability). With this program, the analysis can also be performed with double-gated subpopulations.

Statistical Analyses—We consider an auto-activation level of a sample as significant when the relative reporter level with respect to the BD-Empty/AD-Empty control (CTRL sample) is larger than two times the relative standard deviation of the control sample,

$$\frac{\langle \text{TagBFP}-\text{H}\rangle_{sample}}{\langle \text{TagBFP}-\text{H}\rangle_{CTRL}} - \frac{\langle \text{TagBFP}-\text{H}\rangle_{CTRL}}{\langle \text{TagBFP}-\text{H}\rangle_{CTRL}} > 2s_{rel} \qquad \text{(Eq. 2)}$$

$$\frac{\langle \text{TagBFP}-\text{H}\rangle_{sample}}{\langle \text{TagBFP}-\text{H}\rangle_{CTRL}} > 1 + 2s_{rel}$$

The relative sample standard deviation is given by

$$s_{rel} = \frac{s}{\mu} \qquad \text{(Eq. 3)}$$

where s is the sample standard deviation and μ is the mean value <Tag-BFP-H> averaged over all available experiments; in the case of the CTRL sample we have 12 independent experiments. The sample standard deviation is given by

$$s = \sqrt{\frac{\sum_{i=1}^{n} (\langle \text{TagBFPH}\rangle_i - \mu)^2}{n-1}} \qquad \text{(Eq. 4)}$$

where $<\text{Tag-BFP-H}>_i$ is the Tag-BFP-H population mean of the i-th experiment; n is the total number of experiments.

All interactions of Table I were classified into four different categories according to their reporter level relative to the CTRL sample. The first category contains interactions with a relative reporter level within a margin of 1 s_{rel} of the CTRL sample; the last category embeds the interactions with a margin larger than 3 s_{rel}.

The magnitude of the reporter level varied between different repetitions of the experiment. This is probably because of differences in the transformation efficiency between different batches of competent yeast cells (see supplemental Fig. S6*A*). Differences in transformation efficiency may lead to different copy number of the reporter plasmid. By applying the following two-point normalization, these variations could be attenuated (supplemental Fig. S6*B*):

$$\text{Normalized mean (sample)} = \frac{\langle \text{TagBFP}-\text{H}\rangle_{sample} - \langle \text{TagBFP}-\text{H}\rangle_{CTRL}}{\langle \text{TagBFP}-\text{H}\rangle_{highest\ affinity} - \langle \text{TagBFP}-\text{H}\rangle_{CTRL}} \times 100\% \qquad \text{(Eq. 5)}$$

By definition, the normalized mean of the CTRL sample (= background of the system) is set to 0% when the normalized mean of the couple with the highest affinity, *i.e.* BD-Barstar Y29F/AD-Barnase H102A, is set to 100%. This normalization procedure can be performed with our Python-based program (see Data Availability section).

To test the null hypothesis that the normalized mean of a given couple is larger than the normalized mean of another couple (with lower affinity, Fig. 5*B*), we used a t test with unequal variances (Welch test):

$$t = \frac{\mu_1 - \mu_2}{\sqrt{\frac{s_1}{n_1} + \frac{s_2}{n_2}}} \qquad \text{(Eq. 6)}$$

where $\mu_{1/2}$ and $s_{1/2}$ are the sample means and sample standard deviations of the two couples, respectively; the sample standard deviations are calculated with Eq. 4 (using n and μ of the corresponding couple). The number of experiments, $n_{1/2}$, are given in Fig. 5*B*. The degrees of freedom were calculated with:

$$v = \frac{\left(\frac{s_1}{n_1} + \frac{s_2}{n_2}\right)^2}{\frac{s_1^4}{n_1^2(n_1-1)} + \frac{s_2^4}{n_2^2(n_2-1)}} \qquad \text{(Eq. 7)}$$

and p values were determined for one-tailed distributions. Significant differences in mean values were annotated in Fig. 5*B* with one star ($p < 0.1$), two stars ($p < 0.05$) or three stars ($p < 0.005$).

To judge the strength of the relationship between affinity and normalized reporter level, a Spearman rank test (48) was performed by taking the difference between the order of K_d and the order of relative reporter level. The Spearman correlation coefficient was calculated as follows:

$$r_s = 1 - \frac{6\sum_{i=1}^{n} d_i^2}{n(n^2-1)} \qquad \text{(Eq. 8)}$$

where d_i is the difference in order of the i-th interaction, and n is the total number of interactions.

Finally, the adjusted R^2 was calculated for the fitted functions to describe the relationship between the normalized reporter level and the affinity using the following formula:

$$R^2 = 1 - \left(\frac{\sum_{i=1}^{n} [f_i - \text{NM}_i]^2}{\sum_{i=1}^{n} [\text{NM}_i - \langle \text{NM}\rangle]^2}\right)\left[\frac{n-1}{n-k-1}\right] \qquad \text{(Eq. 9)}$$

where f_i is the normalized reporter level of the i-th interaction when estimated with Eq. S2 (see caption of supplemental Fig. S10). NM_i is the actual normalized reporter level and <NM> is the mean value of the actual reporter levels. The total number of tested interactions (n) and the number of parameters in Eq. S2 (k) are used to correct for the bias in the estimation of R^2.

RESULTS

Auto-activation Impedes the Investigation of Interactions Between Proteins of the Peroxin Family—Auto-activating BD-Bait fusion proteins are a major concern for all yeast-two hybrid approaches (49). Indeed, we detected seven BD-Bait

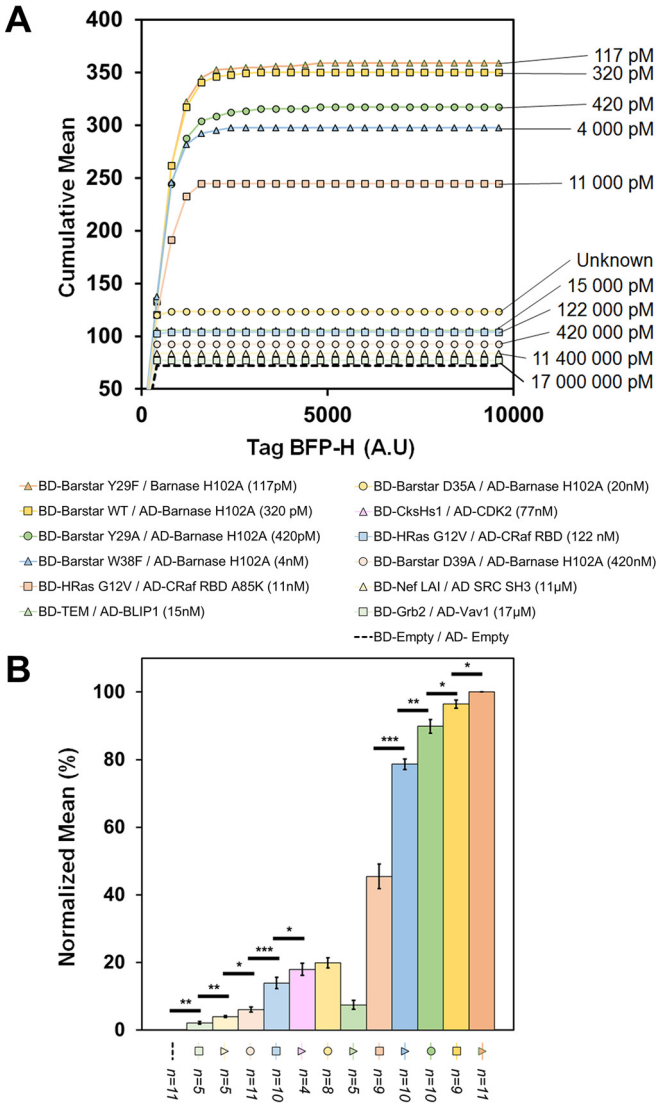

FIG. 5. **qY2H affinity ladder.** The same dual gating approach as in Fig. 4 was applied to the data of all twelve couples of the affinity set (without auto-activation). One million cells were cultured, induced and analyzed. *A.* A representative experiment with eleven couples is shown using raw values. The cumulative mean curves are ordered according to their dissociation constants (Table I). An exception is the BD-TEM/AD-BLIP1 (K_d = 15 nM) couple that displays a too weak cumulative mean. The couple BD-CksHs1/AD-CDK2 is missing in this particular experiment; it was tested at a later stage of this work (during the revision process). Its data is represented as normalized mean in (*B*). *B.* Independent repetitions of the experiments (n = 4 to 11) were used to perform a statistical analysis between direct neighbors of the affinity ladder. The mean value of the Tag-BFP-H channel was normalized as explained in the section "Statistical analyses" of the "Experimental procedures". Error bars are presented as the standard error of the mean (*, p value < 0.05; **, p value < 0.01; ***, p value < 0.001). Without normalization, the (relative) standard errors of the mean are higher for most of the couples (see supplemental Fig. S6). Thus, the significance levels are lower. This analysis confirms that BD-TEM/AD-BLIP1 is weaker than expected. However, with five repetitions of the experiment, we can detect a statistically significant difference between the CTRL sample (BD-Empty/BD-Empty) and the fusion proteins with an elevated auto-activation level (Table II); none of the AD-Prey fusions showed a significant auto-activation level.

The auto-activating BD-Bait fusions were not further considered in our qY2H assay. Fortunately, the probability that both proteins of a PPI cause auto-activation as BD-Bait is rather low. Therefore, most interactions can be studied at least in one orientation. An exception is the interaction between Pex19p and Pex3p. BD-Pex9p, BD-Pex3p and BD-Pex3p W104A featured all elevated auto-activation levels. Thus, two PPIs out of 14 could not be further studied.

In our LexA-based qY2H assay with 2μ plasmids the fusion BD-MNAT1 yielded an auto-activation phenotype (Table II). Previous studies did not encounter this auto-activation problem (41, 42). Thus, the addition of the Tag-RFP may increase the auto-activation potential of certain BD-Baits fusions in LexA-based systems.

qY2H Enables the Monitoring of the Expression Level of the Reaction Partners After 2 h—Initial qY2H reactions were performed with a reduced set of PPIs (BD-Barstar/AD-Barnase H102A as well as BD-HRas G12V/AD-CRaf-RBD, and mutations thereof). Two hours after induction of the Y2H reaction, the expression of all BD-Bait and AD-Prey fusions can be easily detected. Fig. 2*A* displays their fluorescence intensities for a subset of couples. The fluorescence intensity typically spans several orders of magnitude higher than the non-fluorescent controls. However, expression problems can be seen with BD-HRas (Fig. 2*C*), for example. Independent quantification by Western blotting (Fig. 3) shows that the expression level of BD-HRas is indeed impaired. In fact, BD-HRas cannot be detected in the Western blotting. Flow cytometry, on the other hand, indicates a slight shift in the probability distribution for BD-HRas expressing cells (with respect to the negative control, see also supplemental Fig. S3).

Thus, flow cytometry gives an immediate indication on eventual expression problems of the Bait and Prey fusions during acquisition. This contrasts with standard Y2H experiments where the expression level of the BD-Bait and AD-Prey fusions is usually unknown at the time of reporter detection. More laborious Western Blots are usually required to gain this information.

Reporter Level Is Correlated with the Expression Level of the Reaction Partners—Even for the weakest Bait-Prey interaction, the reporter can already be detected two hours after induction. For interactions with K_d-values in the nano- to picomolar range, the gain with respect to the CTRL sample can be clearly detected by eye (Fig. 2). For interactions with micromolar affinity, these gains are much smaller and require a numerical analysis (see below).

PPI with the weakest affinity (BD-Grb2/AD-Vav1). For the couple BD-Barstar D35A/AD-Barnase H102A no dissociation constant is reported in the literature. Our affinity ladder allows to rank the constant between 11 and 77 nM.

TABLE I

List of BD-Bait and AD-Prey couples tested with the qY2H approach. A set of known interactions was generated with proteins pairs with a reported affinity. The dissociation constants (K_d) were taken from the referenced literature and are given in pM; the molecular weights (MW) are in kDa. An additional Specificity Test Set was composed by cross-testing a sub-selection of BD-Bait and AD-Preys fusions of the Affinity Test Set, complemented with the fusions BD-ARMC1, BD-GMPPA, AD-Emerin and AD-MNAT1

Affinity Test Set

Bait proteins						Prey proteins				
Organism	Family	Name	Mutant	MW	K_d	Organism	Family	Name	Mutant	MW
B. amylo-liquefaciens	RNAse inhibitor	Barstar	WT	10	320 [a]	*B. amylo-liquefaciens*	RNAse	Barnase	H102A	12
			Y29A	10	420 [a]					
			Y29F	10	117 [a]					
			W38F	10	4 000 [a]					
			D35A	10	-					
			D39A	10	420 000 [b]					
H. sapiens	GTPase	HRas	G12V C186A	21	122 000 [c]	*H. sapiens*	Kinase	CRaf RBD	WT	9
					11 000 [d]				A85K	9
H. sapiens	Protein kinase regulatory subunit	CksHs1	WT	10	77 000 [e]	*H. sapiens*	Kinase	CDK2	WT	34
E.coli	β-Lactamase	TEM	WT	31	15 000 [f]	*S. clavuligerus*	β-Lactamase inhibitor	BLIP1	WT	21
HIV1	Virulence factor	Nef	LAI	23	11 400 000 [g]	*H. sapiens*	Kinase	SRC SH3	WT	7
H. sapiens	Peroxin	Pex3p	WT Q34-K373	38	3 000 [h]	*H. sapiens*	Peroxin	Pex19p	C8A, C128A, C226A, C229A, C296A	32
			Q34-K373 W104A	38	1 084 000 [h]					
H. sapiens	Adapter	Grb2 SH3	WT	7	17 000 000 [i]	*M. musculus*	Guanine nucleotide exchange factor	Vav1 SH3	WT	8

Specificity Test Set

Bait proteins					Prey proteins				
Organism	Family	Name	Mutant	MW	Organism	Family	Name	Mutant	MW
H. sapiens	Metal ion transport	ARMC1	WT	31	B. amylo-liquefaciens	Rnase	Barnase	H102A	12
B. amylo-liquefaciens	RNAse inhibitor	Barstar	Y29F	10	*H. sapiens*	Kinase	CDK2	WT	34
H. sapiens	Kinase	CksHs1	WT	10	*H. sapiens*	Kinase	CRaf RBD	WT	9
H. sapiens	Phosphorylase	GMPPA	WT	46	H. sapiens	Structural protein	Emerin	WT	29
H. sapiens	Adapter	Grb2 SH3	WT	7	*H. sapiens*	Cell cycle control protein	MNAT1	WT	36
HIV1	Virulence factor	Nef	LAI	23	*H. sapiens*	Peroxin	Pex19p	C8A, C128A, C226A, C229A, C296A	32
E.coli	β-Lactamase	TEM	WT	31	*H. sapiens*	Peroxin	Pex3p	WT Q34-K373	38
					H. sapiens	Kinase	SRC SH3	WT	7
					M. musculus	Guanine nucleotide exchange factor	Vav1 SH3	WT	8

By combining these seven BD- Bait and nine AD- Prey fusions 59 potential negative controls are generated (4 interactions with known affinity are excluded : Barstar Y29F / Barnase H102A, CksHs1/ CDK2, Nef LAI/ SRC, and Grb2 / Vav1). See main text for the selection criteria of these fusion proteins.

[a] ITC, 50 mM Tris/HCl, pH 8 at 25 °C (26).

[b] Mean values from two studies (26, 27) with ITC, 24 mM Hepes, pH 8, 1 mM DTT at 25 °C.

[c] Mean values from four studies of Ras G12V (without the membrane anchor): SPR, 50 mM Tris/HCl, pH 7.4, 100 mM NaCl, 5 mM $MgCl_2$ (28); SPR, 50 mM Tris/HCl, pH 7.4, 100 mM NaCl, 5 mM $MgCl_2$ (29); SPR, 10 mM Hepes, pH 7.4, 150 mM NaCl, 2 mM $MgCl_2$, and 0.01% Nonidet P-40 25 °C (30); ITC, 50 mM Hepes, pH 7.4, 125 mM NaCl, 5 mM $MgCl_2$,25 °C (32).

[d] ITC, 50 mM Hepes, pH 7.4, 125 mM NaCl, 5 mM $MgCl_2$, 25 °C (32). The dissociation constant of the CRaf RBD A85K mutant was measured with HRas WT loaded with a GTP-analogue. The mutant HRas G12V is known to decrease the dissociation constant for the interaction with CRaf RBD WT by a factor of 11 (31). The given value applies the same correction factor.

[e] SPR, 10 mM Hepes, 3.4 mM EDTA, 150 mM NaCl, 0.001% surfactant P20, pH 7.4 (37).

[f] SPR, 10 mM Hepes, 3.4 mM EDTA, 150 mM NaCl, 0.05% surfactant P20, pH 7.4 (33).

[g] ITC, 20 mM phosphate buffer, pH 7.5, 150 mM NaCl, 2 mM EGTA, and 5 mM DTT, 25 °C (34).

[h] SPR, 10 mM Hepes-Na, pH 7.4, 0.15 M NaCl, 3 mM EDTA, and 0.005% (v/v) Tween 20, 25 °C (35).

[i] SPR, 25 °C (36).

TABLE II

Detection of auto-activating proteins. All proteins of Table I were tested as BD-Bait and AD-Prey against the corresponding empty fusion proteins (AD-Empty and BD-Empty, respectively). Their reporter levels were compared to the one of the CTRL sample (BD-Empty/AD-Empty). Based on the ratio <Tag-BFP-H>$_{sample}$/<Tag-BFP-H>$_{CTRL}$, we applied two thresholds to detect significant auto-activation levels. The first threshold used the global population, when the second was based on a double-gated subpopulation (see text). Double gating ensures that auto-activation levels are compared for the same expression levels of BD-Bait and AD-Prey fusion proteins. A significant auto-activation phenotype is characterized by a signal above 1.20 for the global population, or above 1.19 for the double gated subpopulation (see section Statistical Analyses of the Experimental Procedures). Auto-activating fusion proteins are represented in red. N.d. indicates no data

	BD-Protein vs AD-Empty	BD-Empty vs AD-Protein
Barstar Y29F	1.02 [[1.05]]	1.06 [[1.08]]
Barstar WT	0.96 [[0.97]]	1.04 [[1.13]]
Barstar Y29A	0.91 [[0.92]]	0.97 [[1.00]]
Barstar W38F	0.94 [[0.95]]	0.98 [[1.09]]
Barstar D35A	0.93 [[0.92]]	0.99 [[1.03]]
Barstar D39A	1.07 [[1.09]]	1.15 [[1.19]]
Barnase H102A	0.91 [[0.92]]	1.04 [[1.13]]
Myosatin	1.02 [[3.63]]	0.96 [[1.05]]
Fstl3	1.05 [[2.29]]	0.98 [[1.06]]
HRas G12V	0.98 [[1.10]]	1.02 [[1.09]]
CRaf RBD WT	1.22 [[1.19]]	1.03 [[1.11]]
CRaf RBD A85K	1.27 [[1.11]]	1.02 [[1.03]]
CDK2	1.03 [[1.14]]	1.01 [[1.04]]
CksHs1	1.04 [[1.04]]	0.97 [[0.97]]
TEM	0.94 [[0.98]]	0.94 n.d.
BLIP1	0.94 [[1.14]]	0.96 n.d.
Nef LAI	1.12 [[1.15]]	1.05 [[1.18]]
SRC SH3	1.26 [[1.18]]	0.91 [[0.94]]
Pex3p	1.03 [[1.22]]	0.93 [[0.98]]
Pex3p W104A	1.04 [[1.31]]	0.94 [[0.97]]
Pex19p	3.36 [[2.704]]	0.94 [[0.98]]
Grb2	0.96 [[1.01]]	0.93 [[0.97]]
Vav1	1.04 [[1.00]]	0.94 [[0.98]]
ARMC1	0.96 [[1.11]]	0.96 [[1.00]]
Emerin	0.94 [[0.98]]	0.94 [[0.99]]
MNAT1	1.02 [[1.61]]	0.95 [[0.99]]
GMPPA	0.94 [[0.98]]	0.94 [[0.99]]

[[…]] = Double gated population:
Tag RFP-H [700-900]; yEGFP-H [5000-6000].

From the visualization of the expression levels, we observe that the reporter level (*i.e.* blue fluorescence intensity) is correlated with the green and red fluorescence intensity: more reaction partners (*i.e.* higher amount of interacting BD-Bait and AD-Prey fusions) yielded more product (reporter). This obvious correlation has consequences for the extraction of quantitative information on the strength of PPIs as we demonstrate later. In the case of the Bait/Prey-couple BD-B112/AD-Barnase H102A (Fig. 2*F*) this correlation is basically only observed for the red fluorescence (BD-Bait). The B112 acid blob acts as an activation domain (50, 51) so that this specific BD-Bait fusion is a functional transcription factor by itself that does not depend on the AD-Prey fusion.

Standardization of BD-Bait and AD-Prey Levels Is Required to Gain Information on Binding Strength—In all repetitions of the experiment, the reporter level of the global cell population roughly reflects the magnitude of the (*in vitro*) affinity. As shown in Fig. 4*A* for a single experiment and a small subset of PPIs, the Bait-Prey couples with high affinity ($K_d \sim$ pM) could be easily distinguished from medium-affinity couples ($K_d \sim$ nM) based on their mean reporter level. It confirms results of previous studies that the global Y2H read-out correlates with *in vitro* affinity (15, 16, 13, 17, 18). In addition, our approach discloses the influence of the expression levels of the reaction partners, *i.e.* the BD-Bait and AD-Prey fusions. Their levels may vary significantly between the studied couples (Fig. 2 and

3) and to a smaller extent between different experiments. These variations complicate the discrimination of Bait-Prey couples based on their affinities. Fig. 4*A* presents a particularly illustrative experiment: The couple BD-HRas/AD-CRaf displays a 20 times lower *in vitro* K_d-value than the couple BD-Barstar D39A/AD-Barnase H102A. Yet the mean reporter level (Fig. 4*A*, right column) is lower for the former couple than for the latter couple; the opposite would have been expected according to the *in vitro* affinities. We note, however, that the former couple exhibits a significant lower expression level of the BD-Bait fusion (Fig. 4*A*, left column) than the latter. Thus, can quantitative information on the strength of the interaction (*i.e.* relative affinities) be reliably extracted from such an experiment?

To address this question, we tried to correct for differences in the expression level by sub-selecting (gating) only cells that display a red and green fluorescence intensity within a certain narrow interval (see Fig. 4*B* and 4*C*). And indeed, when standardizing the red fluorescence intensity (*i.e.* gating for cells with similar BD-Bait expression level), the mean reporter level reflects the *in vitro* affinities for the two couples BD-HRas/AD-CRaf and BD-Barstar D39A/AD-Barnase H102A (Fig. 4*B*). Similarly, the couple BD-Barstar Y29F/AD-Barnase H102A has the lowest AD-Prey expression level and displays a weaker reporter level than expected. Standardization of the AD-Prey level corrects the reporter levels of the studied couples according to their reported *in vitro* affinities (Fig. 4*C*). Changing the location of the gating intervals leads to the same conclusions (see supplemental Fig. S4) but the number of analyzed cells can be affected. The gates used in Fig. 4 provided us with the sensitivity to easily detect the weakest PPI of the subset. Also, these gates yielded the necessary resolution to clearly separate all PPIs.

A Reproducible Affinity Ladder Can Be Generated for PPIs with a K_d Between 100 pM and 20 μM—To setup our qY2H system, we used a reduced set of PPIs (Fig. 2 and 4). For these setup experiments, exhaustive samples sizes of ten million cells were cultured, induced and analyzed. To improve the throughput, we determined the minimal number of cells required to achieve a robust estimate of the reporter level. It turned out that a subsample of at least one million cells is required (see supplemental Fig. S5) to match the result of the entire sample.

Finally, we challenged the previously defined settings (two hours of reaction, one million cells and the standardization gates of Fig. 4) with the eleven PPIs of the Affinity Test Set. As a result, we obtained the affinity ladder of Fig. 5*A* where the couples are ordered accordingly to their measured *in vitro* affinity. An exception is the couple BD-TEM/AD-BLIP1 that is ranked too low. The results for the couple BD-CksHs1/AD-CDK2 are missing in Fig. 5*A*. This couple was added during the revision of this article; the results are presented in Fig. 5*B*.

The ordering of the couples does not change when different repetitions of the experiment are compared (supplemental Fig. S7*A*). An exception is again the couple BD-TEM/AD-BLIP that displays a high variability. Also, couples with very similar affinities (*i.e.* BD-Barstar WT/AD-Barnase H102A with 320 pM and BD-Barstar Y29A/AD-Barnase H102 with 420 pM) can be ordered incorrectly in certain experiments. However, when the normalized reporter level (see Experimental Procedures) is averaged over five repetitions of the qY2H experiment, these two couples are ordered correctly (see supplemental Fig. S7*C*). Moreover, we observed significant differences between all neighbors of our affinity ladder but one. It is the interaction with the weakest affinity (K_d = 17 μM, BD-Grb2/AD-Vav1). By increasing the number of repetitions, significant differences can be obtained also for this couple (supplemental Fig. S7*C*).

In conclusion, eleven out of twelve pairs of the ATS are ordered correctly (Fig. 5*B*); this corresponds to a Spearman rank correlation coefficient of 0.96. It validates the qY2H system's capability of ranking the PPIs of Table I based on their affinities. However, the qY2H seems to be limited to interactions with a $K_d < 20$ μM.

Affinity Ladder Permits Rapid Classification of PPIs Based on Their Strength—Often the goal is to rank PPIs based on their affinity or to obtain an upper and lower bound for the dissociation constant. The above affinity ladder can be used for a rapid visual classification of PPIs with thus far unknown affinities within a given range (here from micro- to picomolar). This is demonstrated at the example of the mutation D35A of Barstar. Thus far, no *in vitro* affinity data is available for the interaction of this mutant with Barnase H102A. With the affinity ladder of Fig. 5*B* we can rank the affinity between those of BD-CksHs1/AD-CDK2 (77 nM) and BD-HRas/BD-CRaf A85K (11 nM).

Our qY2H experiment indicates that the Barstar mutant D35A exhibits a significantly higher affinity for Barnase H102A than the Barstar mutant D39A (420 nM). To validate this observation, we performed independent alchemical free-energy calculations (see Suppl. Material). Through the use of a thermodynamic cycle (supplemental Fig. S8*A*) we calculated the difference in binding free energy between the mutants Barstar D35A and Barstar D39A. We obtained a value of -1.9 ± 0.3 kcal/mol which indicates that the dissociation constant of the mutant D35A is about 20 times lower than that of the mutant D39A. Thus, we can estimate a dissociation constant of about 20 nM for the mutant D35A in agreement with the qY2H experiment.

The Specificity Test Set Generates Seven Positives Out of 59—When the qY2H system was challenged with 59 potential negative controls, we found 52 pairs within the error margin of the CTRL sample BD-Empty/AD-Empty (supplemental Fig. S9). The nine pairs with the highest relative reporter level (including seven positive pairs) have the BD-ARMC1 fusion in common. Despite this fusion did not display any auto-activa-

tion phenotype (Fig. 2), it seems to cause nonspecific positives (with proteins from eight different families).

The strongest signal of the STS was obtained when BD-ARMC1 was paired up with AD-Emerin. Interestingly, this orientation produced a negative phenotype in five different GAL4-based Y2H assays (42). The reverse orientation yielded in our qY2H system a reporter level within the error margin of the CTRL sample (supplemental Fig. S2) like in six out of nine GAL4-based Y2H assays (41, 42). Taking together these results, we conclude that ARMC1 is error prone when used as BD-Bait in our LexA-based Y2H system and therefore seems not to be a suited candidate for testing the specificity of qY2H assays in the future.

Concerning the protein MNAT1, we were forced to use it as Prey because of an auto-activation phenotype of BD-MNAT1 (Fig. 2). Except with BD-ARMC1 (see above), AD-MNAT1 does not generate any positive signal with the tested BD-Bait fusions, including BD-GMPPA. The negative result with the latter coupler agrees with Ref (42).

In conclusion, the fusions of the STS (except BD-ARMC1) are well suited candidates to evaluate the specificity of future qY2H experiments.

DISCUSSION

Quantitative Features of the Tri-fluorescent Yeast Two-hybrid System—The tri-fluorescent qY2H system offers the novelty of identifying expression correlations for the genes involved in the actual Y2H reaction. For true positive interactions the reporter level is correlated with both reaction partners. For false positive interactions where the Bait acts as activation domain (*e.g.* BD-B112), the reporter level is basically only correlated with one reaction partner. This characteristic correlation pattern can serve as additional criteria to discriminate such false positive interactions from true positives. It complements the auto-activation test with proper controls (*i.e.* empty Bait and Prey plasmids) routinely applied in Y2H assays. The visual recognition of this pattern requires, however, a relatively strong reporter level (*i.e.* about three times higher than the CTRL sample).

Our qY2H system, like all yeast two hybrid assays is faced to the problem of auto-activating proteins (49). However, most of the auto-activating phenotypes that we have detected can be attributed most likely to the intrinsic properties of the tested proteins. They can interact/modulate the transcription machinery. For example, it has been reported that SRC interacts and modulates Hepatocyte Nuclear Factor-1 (52) and TFII-I (53), when MNAT1 can recognize Octamer Transcription Factors via their POU domain (54). Moreover, proteins of the Pex family from *Saccharomyces cerevisiae* have been demonstrated to interact with the TATA Binding Protein 1 (55). For CRaf RBD there is no reasonable explanation for its elevated auto-activation level. Fortunately, the probability that both proteins of a PPI cause an elevated auto-activation level as BD-Bait is rather low.

In the past, significant effort has been spent to render the Y2H read-out quantitative and thereby gain quantitative information on the strength of interactions (see cited literature in the Introduction). Our study clearly demonstrates that the quantification of the reaction partners is important, too. We have shown that variations in the expression levels of BD-Bait and AD-Prey can lead to reporter levels that are not ordered according to the underlying PPI affinities. Through a simple gating process, it is, however, possible to standardize the expression levels of BD-Bait and AD-Prey and thereby overcome this difficulty.

From our studies it seems that the qY2H system reaches saturation for interactions with a K_d below 100 pM. However, only mutations of the same couple (Barstar/Barnase H102A) were tested in this region. To better define this limit, other types of PPIs should be tested in the future. The lower limit seems to be at 20 μM with the current experimental conditions. Within the range 100 pM to 20 μM, we see a high correlation between the normalized reporter level and the affinity (see supplemental Fig. S10). The relationship follows a classical dose-response curve that can be well fitted with standard sigmoid-like functions. Such fitted functions may improve in the future the estimation of the K_d for interactions with unknown affinities. For example, for the couple Barstar D35A/Barnase H102A we estimated a value between 18 and 49 nM which is a slightly narrower range than the one imposed by the ladder approach (between 11 nM and 77 nM). Nevertheless, depending on the data set, different parameters can be obtained for the fitted functions (explaining the range of predictions, see also caption of supplemental Fig. S10). More data will be necessary to consolidate this fitting strategy. For the moment we consider the ladder approach the more cautious strategy.

In cellula Is Not In Vitro—The observed agreement between *in cellula* reporter levels and *in vitro* affinities (Fig. 5*B* and supplemental Fig. S10) cannot be presumed *a priori*. The *in vitro* experiment measures the affinity between the interactors alone (or with tags) whereas the qY2H system relies on fusion proteins (Fig. 1). If the fused domains influence the interaction between the Bait and Prey, *e.g.* by blocking the binding interface, the resulting *in cellula* reporter level would be impaired and most likely not correlate with the *in vitro* affinity.

We have designed our fusion proteins so that Bait and the Prey are located at the C-terminus. Consequently, there is only a single hinge joint between the Bait and the remaining LexA-RFP fusion or between the Prey and the B42-GFP fusion. This should minimize the number of possible intra-molecular interactors that can block the binding site. Nevertheless, steric hindrance effects may still influence the accessibility of the binding interface. This could explain why two out of twelve interactions (Barstar/Barnase and CDK2/CksHs1) displayed significantly different reporter levels when tested in the two possible orientations (supplemental Fig. S2).

TABLE III
Sensitivity and specificity of the qY2H. Benchmarks are given for the Affinity Test Set and the Specificity Test Set

	Total	Positive	Statistically significant with at least 5 repetitions	Negative	Auto-activation phenotype in both orientations
Affinity Test Set	14	11	12	0	2
Specificity Test Set	59	7*		52	

*All positive pairs were obtained with BD-ARMC1.

Most interactions yielded, however, only slightly different reporter levels in the two orientations.

Beside steric hindrance effects, the distance between BD and AD (and their relative orientation) can vary depending on the studied BD-Bait/AD-Prey complex. As a result, the efficiency of the transcription cannot be assumed *a priori* to be equal for different types of proteins. Similar effects can apply to *in vitro* approaches with immobilized bio-molecules, like SPR. Thus, orientation/accessibility problems can generate discrepancies between the various methods to measure affinities *in vitro* and *in cellula*.

In vitro experiments measure the affinity under well-defined buffer-controlled equilibrium conditions. In contrast, our *in-cellula* experiments take place in non-equilibrium microvessels (56) where the interaction partners can interact with the endogenous complex solution of biomolecules. This may lead to effectively smaller concentrations of the reaction partners. Also, post-translational modification(s) could impact the interactions.

When averaged over five repetitions of the qY2H experiment, all couples can be ranked according to their *in vitro* affinity (supplemental Fig. S7C). An exception is the interaction between TEM and BLIP1. Interestingly, this PPI displayed a remarkable variability of interaction strengths in the *in vitro* experiments. The K_d varied from 400 to 15,000 pM depending on the buffer (at a constant pH of 7.5) (33). Moreover, a high dependence on the pH has been reported: by increasing the pH from 7.5 to 8.5 the dissociation constant is multiplied by a factor 100 (33). The other couples of Table I do not display such strong variations to the best of our knowledge. The pH-dependence of PPIs can of course impact the result of the qY2H experiment. The nucleus is more basic than the cytoplasm. Values up to pH 8 have been reported (57). Also, the reported conditions for *in vitro* assays with yeast RNA polymerases recommend a pH-value of 8 (58). In such an environment, the observed affinity between TEM and BLIP1 is much weaker than the value given in Table I (for pH 7.5 in Hepes buffer as for most of the couples). Indeed, this was observed in our qY2H experiment. The difference between the nuclear environment and standard buffer conditions for *in vitro* experiments could explain why some interactions can only be observed with yeast two-hybrid. This might be especially relevant for proteins with optimized functioning in the nucleus.

With prior knowledge about the Bait or Prey the amino acid sequence can be optimized to take into account their intrinsic properties, like specific sub-cellular localization. An illustrative example is the protein HRas, which is usually found to be associated to the cytoplasmic membrane through its C-terminal anchor. Mutation of C186A abolishes the anchor function (59) and the protein can be used for the *in cellula* measurements.

Table III presents the sensitivity and specificity benchmarks of the qY2H system in the light of its caveats as an *in cellula* assay. With a single repetition of the experiment, the qY2H system was able to detect eleven interactions with known affinity out of 14. An additional couple (with the weakest affinity) generates a reporter level distinguishable from the system's background when studied at least five times. The two remaining couples cannot be studied because of an auto-activation phenotype in both orientations. Thus, our system can detect 86% of the tested interactions with known affinity when including auto-activating couples as failures, and 100% otherwise. The STS generated seven positive signals (12%), all with the BD-ARMC1 fusion in common.

Workload and Scalability—The qY2H approach has been designed to standardize expression levels of the reaction partners and thereby estimate the *in cellula* affinity of PPIs. Its throughput cannot be compared with binary Y2H assays that aim to give a YES/NO answer such as the CrY2H-seq approach (60). With respect to current *in vitro* or *in cellula* methods for the measurement of the affinity of PPIs, our qY2H assay can, however, be considered as a high-throughput approach. When studying specific PPI couples, as we did in this work, the limiting step in terms of time and financial resources is the construction of the plasmids (some with optimized coding sequence, see for example HRas). Once amplified plasmids were available, up to eight complete qY2H experiments with 24 samples could be performed within one month and a workload of 0.5 man-month. This throughput is based on our experience during the setup phase of the qY2H approach when we tested different experimental conditions. Thus, about 40 couples can in principle be characterized (including the auto-activation and orientation filters and five repetitions of the experiments) within one month by a single manipulator. The throughput of all steps of the protocol (except data acquisition by flow cytometry) can be scaled linearly with increasing manpower. As these steps have been optimized for liquid phase, a scale-up with robots could even be envisaged (61). The acquisition by flow cytometry might be also a limiting step

for the scalability. With the MACSQuant VYB flow cytometer used in this work, a maximum of 100 samples can be measured per day (with a flow speed of 16,000 events/s). With more advanced equipment such as the MACSQuant X, about 8000–10,000 samples can be measured per day.

Recommendations—Beside potential sequence optimizations (as proposed above), we recommend the following precautions to be taken for the measurement with the qY2H system:

1. As in any Y2H screen, BD-Bait and AD-Prey constructs should be tested against controls, *i.e.* AD-Empty and BD-Empty, respectively, to identify auto-activating BD-Bait or AD-Prey fusion proteins. For comparison reasons, the CTRL sample must be measured, too. It is also required to remove the background of the system when calculating normalized means.

2. The PPIs should be tested in both orientations, *i.e.* with the proteins switched between the Bait and Prey vectors, to identify the orientation with the higher reporter level (for standardized levels of reaction partners).

3. We recommend to pre-transform BD-Bait-expressing haploids with the reporter plasmid. It increases the reporter level. Two subsequent transfections are more efficient than a single double transfection. Use only freshly transformed yeast cells for the qY2H experiment. Storing diploids yeast cells for a week in the refrigerator decreases the level of AD-Prey and reporter level by a factor two to five.

4. For the construction of the affinity ladder, the gating interval for the red fluorescence intensity (BD-Bait) was positioned at the lowest possible location to avoid saturation effects, *i.e.* it was set just above the 95% threshold of the non-fluorescent cells. Also, a low expression level of the BD-Bait limits auto-activation effects. The gating intervals of the green fluorescence intensity was set to a medium range value to reach the desired sensitivity but to avoid saturation and protein burden effects (62). The width of each interval gate should not be larger than 20–30% of the value of its lower border. It narrows the variations in concentration of BD-Bait and AD-Prey among the studied cells.

5. If the gating intervals are not directly applied at acquisition time on the flow cytometer, at least 10^6 cells should be acquired for analysis. This number is sufficient to reach a converged ladder after gating (see supplemental Fig. S5). For this number of cells cultures of 10 ml are enough.

6. In all repetitions of the qY2H experiment, the two couples with the lowest affinity (BD-Nef LAI/AD-SRC and BD-Grb2/AD-Vav1) displayed a higher reporter level than the CTRL sample. This difference was, however, smaller than twice the relative sample standard deviation of the CTRL sample. Thus, with a single experiment, the qY2H system reaches its detection limit for PPIs with a K_d of about 20 μM (and higher). To obtain statistically significant results for such weak interactions, we recommend repeating the experiment (with associated controls).

CONCLUSION

The newly constructed vectors provide for the first time access to a quantitative Y2H system with fluorescent tags for the reaction partners (BD-Bait, AD-Prey) *and* the reporter. The established protocol is rapid, sensitive and highly reproducible (when using normalized reporter levels). It permits easy detection of expression problems of the reaction partners. Using flow cytometry, the expression levels of the reaction partners can be monitored cell by cell simultaneously with the level of the reporter. The single-cell data can be exploited to identify correlation patterns as indicators of physical interactions.

The qY2H method presented in this work offers also an approach to quantitative data on the strength of protein-protein interactions in living cells. In this context, we have demonstrated the importance of quantifying the product *and* the reaction partners of the Y2H reaction: standardization is critical to correct for differences in expression levels between couples. Using a straightforward gating analysis, an affinity ladder can be easily generated that permits rapid classification of PPIs according to their affinity. We would like to emphasize, however, that these *in cellula* affinities are effective quantities that depend on the cell's complex microenvironment; and this environment may change as a function of the yeast strain and the experimental conditions (temperature, medium, *etc*).

Our qY2H approach is an ideally suited tool to complement cross-mating approaches (61, 63) with libraries of yeast clones. Once PPI candidates have been identified with standard high-throughput Y2H screens, the interaction strength of key players of the PPI network can be estimated with our approach. Thus, quantitative PPI networks can be created by attributing weights to the PPI edges according to their *in-cellula* affinity. The topology of force-directed networks may help identifying key pathways within the network, and how these paths change as a function of environmental conditions (stress, metabolism, *etc*). Thus, we anticipate that qY2H data would boost the modeling of interactomes and thereby advance significantly systems biology.

Acknowledgments—We thank Dr Francesca Palladino and Matthieu Caron for technical support on the Western blots and Dr Gaël Yvert for helpful comments on the manuscript.

DATA AVAILABILITY

Our Python-based program for the automated generation of the qY2H affinity ladder (with a graphical user interface) can be downloaded here: http://github.com/LBMC/qY2H-Affinity-Ladder. The minimal requirements and installation instructions are given in the user guide (see supplemental Material).

The flow cytometry files of the experiment shown in Fig. 4 and Fig. 5*A* can be downloaded from http://flowrepository.org under accession number FR-FCM-ZYUL and FR-FCM-Z25G.

Other experimental data can be provided upon request.

http://flowrepository.org/id/FR-FCM-ZYUL

http://flowrepository.org/id/FR-FCM-Z25G

* This project was supported by a grant from the Fond Recherche of the ENS de Lyon. We are grateful to the Pôle Scientifique de Modélisation Numérique (Lyon, France) for computer time, and the SFR Biosciences Gerland-Lyon Sud (UMS344/US8) for the access to the MacsQuantVYB flow cytometer. The authors declare that they have no conflicts of interest with the contents of this article.

[S] This article contains supplemental Figures, Tables, and Data.

‡ To whom correspondence should be addressed. Tel.: +33 472 72 8645; E-mail: martin.spichty@ens-lyon.fr.

Author contributions: D. Cluet and M.S. designed research; D. Cluet, I.A., B.V., J.L., A.A., C.G., and M.S. performed research; D. Cluet, I.A., J.L., and D. Calabrési contributed new reagents/analytic tools; D. Cluet, I.A., and M.S. analyzed data; D. Cluet and M.S. wrote the paper.

REFERENCES

1. Vogelstein, B., Lane, D., and Levine, A. J. (2000) Surfing the p53 network. *Nature* **408,** 307–310
2. Feng, Y., and Walsh, C. A. (2001) Protein–Protein interactions, cytoskeletal regulation and neuronal migration. *Nat. Rev. Neurosci.* **2,** 408–416
3. Takenawa, T., and Suetsugu, S. (2007) The WASP–WAVE protein network: connecting the membrane to the cytoskeleton. *Nat. Rev. Mol. Cell. Biol.* **8,** 37–48
4. Scott, J. D., and Pawson, T. (2009) Cell signaling in space and time: where proteins come together and when they're apart. *Science* **326,** 1220–1224
5. Barabási, A. L., and Oltvai, Z. N. (2004) Network biology: understanding the cell's functional organization. *Nat. Rev. Genet.* **5,** 101–113
6. Fields, S., and Song, O. (1989) A novel genetic system to detect protein–protein interactions. *Nature* **340,** 245
7. Gyuris, J., Golemis, E., Chertkov, H., and Brent, R. (1993) Cdi1, a human G1 and S phase protein phosphatase that associates with Cdk2. *Cell* **75,** 791–803
8. Stynen, B., Tournu, H., Tavernier, J., and Van Dijck, P. (2012) Diversity in genetic in vivo methods for protein-protein interaction studies: from the yeast two-hybrid system to the mammalian split-luciferase system. *Microbiol. Mol. Biol. Rev.* **76,** 331–382
9. Chen, J., Zhou, J., Bae, W., Sanders, C. K., Nolan, J. P., and Cai, H. (2008) A yEGFP-based reporter system for high-throughput yeast two-hybrid assay by flow cytometry. *Cytometry A* **73A,** 312–320
10. Yachie, N., Petsalaki, E., Mellor, J. C., Weile, J. , Jacob, Y., Verby, M., Ozturk, S. B., Li, S., Cote, A. G., Mosca, R., Knapp, J. J., Ko, M., Yu, A., Gebbia, M., Sahni, N., Yi, S., Tyagi, T., Sheykhkarimli, D., Roth, J. F., Wong, C., Musa, L., Snider, J., Liu, Y. C., Yu, H., Braun, P., Stagljar, I., Hao, T., Calderwood, M. A., Pelletier, L., Aloy, P., Hill, D. E., Vidal, M., and Roth, F. P. (2016) Pooled-matrix protein interaction screens using Barcode Fusion Genetics. *Mol. Syst. Biol.* **12,** 863–863
11. Parrish, J. R., Gulyas, K. D., and Finley, R. L. (2006) Yeast two-hybrid contributions to interactome mapping. *Curr. Opin. Biotechnol.* **17,** 387–393
12. Vidal, M., and Fields, S. (2014) The yeast two-hybrid assay: still finding connections after 25 years. *Nat. Methods* **11,** 1203–1206
13. Estojak, J., Brent, R., and Golemis, E. A. (1995) Correlation of two-hybrid affinity data with in vitro measurements. *Mol. Cell. Biol.* **15,** 5820–5829
14. Fields, S. (1993) The two-hybrid system to detect protein-protein interactions. *Methods* **5,** 116–124
15. Möckli, N., and Auerbach, D. (2004) Quantitative β-galactosidase assay suitable for high-throughput applications in the yeast two-hybrid system. *BioTechniques* **36,** 5
16. Wagemans, J., and Lavigne, R. (2015) Identification of protein-protein interactions by standard gal4p-based yeast two-hybrid screening. In *Protein-Protein Interactions* (C. L. Meyerkord, H. Fu, Eds.), pp. 409–431, Springer New York, New York, NY
17. Colas, P., Cohen, B., Ferrigno, P. K., Silver, P. A., and Brent, R., (2000) Targeted modification and transportation of cellular proteins. *Proc. Natl. Acad. Sci. U.S.A.* **97,** 13720–13725
18. Hu, X., Kang, S., Chen, X., Shoemaker, C. B., and Jin, M. M. (2009) Yeast surface two-hybrid for quantitative *in vivo* detection of protein-protein interactions via the secretory pathway. *J. Biol. Chem.* **284,** 16369–16376
19. Younger, D., Berger, S., Baker, D., and Klavins, E. (2017) High-throughput characterization of protein–protein interactions by reprogramming yeast mating. *Proc. Natl. Acad. Sci. U.S.A.* **114,** 12166–12171
20. Zolghadr, K., Mortusewicz, O., Rothbauer, U., Kleinhans, R., Goehler, H., Wanker, E. E., Cardoso, M. C., and Leonhardt, H. (2008) A fluorescent two-hybrid assay for direct visualization of protein interactions in living cells. *Mol. Cell. Proteomics* **7,** 2279–2287
21. Yurlova, L., Derks, M., Buchfellner, A., Hickson, I., Janssen, M., Morrison, D., Stansfield, I., Brown, C. J., Ghadessy, F. J., Lane, D. P., Rothbauer, U., Zolghadr, K., and Krausz, E. (2014) The fluorescent two-hybrid assay to screen for protein–protein interaction inhibitors in live cells: targeting the interaction of p53 with Mdm2 and Mdm4. *Biomol. J. Screen.* **19,** 516–525
22. Jeong, K. J., Seo, M. J., Iverson, B. L., and Georgiou, G. (2007) APEx 2-hybrid, a quantitative protein-protein interaction assay for antibody discovery and engineering. *Proc. Natl. Acad. Sci.* **104,** 8247–8252
23. Dutta, S., Koide, A., and Koide, S. (2008) High-throughput analysis of the protein sequence–stability landscape using a quantitative yeast surface two-hybrid system and fragment reconstitution. *J. Mol. Biol.* **382,** 721–733
24. H. Endoh, A. J. M. Walhout, M. Vidal, (2000) [6] A green fluorescent protein-based reverse two-hybrid system: Application to the characterization of large numbers of potential protein-protein interactions, in *Applications of Chimeric Genes and Hybrid Proteins - Part C: Protein-Protein Interactions and Genomics*, Methods Enzymol., J. Thorner, S. D. Emr, J. N. Abelson, Eds. (Academic Press, 2000), pp. 74-IN1
25. Starling, A. L., Ortega, J. M., Gollob, K. J., Vicente, E. J., Andrade-Nóbrega, G. M., and Rodriguez, M. B. (2003) Evaluation of alternative reporter genes for the yeast two-hybrid system. *Genet. Mol. Res.* **2,** 124–135
26. Schreiber, G., and Fersht, A. R. (1995) Energetics of protein-protein interactions: Analysis ofthe Barnase-Barstar interface by single mutations and double mutant cycles. *J. Mol. Biol.* **248,** 478–486
27. Frisch, C., Schreiber, G., Johnson, C. M., and Fersht, A. R. (1997) Thermodynamics of the interaction of barnase and barstar: changes in free energy versus changes in enthalpy on mutation. *J. Mol. Biol.* **267,** 696–706
28. Herrmann, C., Horn, G., Spaargaren, M., and Wittinghofer, A. (1996) Differential interaction of the Ras family GTP-binding proteins H-Ras Rap1A, and R-Ras with the putative effector molecules Raf kinase and Ral-guanine nucleotide exchange factor. *J. Biol. Chem.* **271,** 6794–6800
29. Block, C., Janknecht, R., Herrmann, C., Nassar, N., and Wittinghofer, A. (1996) Quantitative structure-activity analysis correlating Ras/Raf interaction in vitro to Raf activation in vivo. *Nat. Struct. Mol. Biol.* **3,** 244–251
30. Fischer, A., Hekman, M., Kuhlmann, J., Rubio, I., Wiese, S., Rapp, U. R. (2007) B- and C-RAF display essential differences in their binding to Ras: the isotype-specific N terminus of B-RAF facilitates Ras binding. *J. Biol. Chem.* **282,** 26503–26516
31. Kiel, C. (2003) Untersuchung von Ras/Effektor-Komplexen mit gezielt veränderten elektrostatischen Eigenschaftens, Dissertation Ruhr-Universität Bochum Fachbereich Biochemie
32. Kiel, C., Filchtinski, D., Spoerner, M., Schreiber, G., Kalbitzer, H. R., and Herrmann, C. (2009) Improved binding of Raf to Ras·GDPIs correlated with biological activity. *J. Biol. Chem.* **284,** 31893–31902
33. Albeck, S., and Schreiber, G., (1999) Biophysical characterization of the interaction of the β-Lactamase TEM-1 with its protein inhibitor BLIP †. *Biochemistry* **38,** 11–21
34. Arold, S., O'Brien, R., Franken, P., Strub, M. P., Hoh, F., Dumas, C., and Ladbury, J. E. (1998) RTLoop Flexibility enhances the specificity of src family SH3 domains for HIV-1 Nef † ‡. *Biochemistry* **37,** 14683–14691
35. Sato, Y., Shibata, H., Nakano, H., Matsuzono, Y., Kashiwayama, Y., Kobayashi, Y., Fujiki, Y., Imanaka, T., and Kato, H. (2008) Characterization of the interaction between recombinant human peroxin Pex3p and Pex19p: Identification of Trp-104 Inpex3p as a critical residue for the interaction. *J. Biol. Chem.* **283,** 6136–6144
36. Nishida, M. (2001) Novel recognition mode between Vav and Grb2 SH3 domains. *EMBO J.* **20,** 2995–3007
37. Bourne, Y., Watson, M. H., Hickey, M. J., Holmes, W., Rocque, W., Reed, S. I., and Tainer, J. A. (1996) Crystal structure and mutational analysis of the human CDK2 kinase complex with cell cycle–regulatory protein CksHs1. *Cell* **84,** 863–874
38. Golemis, E. A., Serebriiskii, I., Finley, R. L. Jr, Kolonin, M. G., Gyuris, J., and Brent, R. (2000) Interaction trap/two-hybrid system to identify interacting proteins. *Curr. Protoc. Cell Biol.* **8,** 17.3.1–17.3.42

39. Genové, G., Glick, B. S., and Barth, A. L. (2005) Brighter reporter genes from multimerized fluorescent proteins. *BioTechniques* **39,** 814–822
40. Shearin, H. K., Macdonald, I. S., Spector, L. P., and Stowers, R. S. (2014) Hexameric GFP and mCherry reporters for the *Drosophila* GAL4, Q, and Lex A transcription systems *Genetics* **196,** 951–960
41. Braun, P., Tasan, M., Dreze, M., Barrios-Rodiles, M., Lemmens, I., Yu, H., Sahalie, J. M., Murray, R. R., Roncari, L., de Smet, A. S., Venkatesan, K., Rual, J. F., Vandenhaute, J., Cusick, M. E., Pawson, T., Hill, D. E., Tavernier, J., Wrana, J. L., Roth, F. P., and Vidal, M. (2009) An experimentally derived confidence score for binary protein-protein interactions. *Nat. Methods* **6,** 91–97
42. Rajagopala, S. V., and Uetz, P. Analysis of Protein–Protein Interactions Using High-Throughput Yeast Two-Hybrid Screens, in *Network Biology*, G. Cagney, A. Emili, Eds. (Humana Press, 2011), pp. 1–29
43. Ma, H., Kunes, S., Schatz, P. J., and Botstein, D. (1987) Plasmid construction by homologous recombination in yeast. *Gene* **58,** 201–216
44. OKevin, R., Vo, K. T., Michaelis, S., and Paddon, C. (1997) Recombination-mediated PCR-directed plasmid construction in vivo in yeast. *Nucleic Acids Res.* **25,** 451–452
45. Foiani, M., Marini, F., Gamba, D., Lucchini, G., and Plevani, P. (1994) The B subunit of the DNA polymerase alpha-primase complex in Saccharomyces cerevisiae executes an essential function at the initial stage of DNA replication. *Mol. Cell Biol.* **14,** 923
46. Gietz, R. D., and Schiestl, R. H. (2007) Frozen competent yeast cells that can be transformed with high efficiency using the LiAc/SS carrier DNA/PEG method. *Nat. Protoc.* **2,** 1
47. Bagwell, C. B. (2005) Hyperlog-A flexible log-like transform for negative, zero, and positive valued data. *Cytometry A* **64A,** 34–42
48. Bailey, D. E. (1971) Probability and statistics, models for research. John Wiley & Sons, Hoboken, New Jersey
49. Mehla, J., Caufield, J. H., Sakhawalkar, N., and Uetz, P. (2017) A comparison of two-hybrid approaches for detecting protein–protein interactions. *Methods Enzymol.* **586,** 333–358
50. Golemis, E. A., and Brent, R. (1992) Fused protein domains inhibit DNA binding by LexA. *Mol. Cell Biol.* **12,** 3006–3014
51. Bickle, M. B. T., Dusserre, E., Moncorgé, O., Bottin, H., and Colas, P. (2006) Selection and characterization of large collections of peptide aptamers through optimized yeast two-hybrid procedures. *Nat. Protoc.* **1,** 1066–1091
52. Soutoglou, E., Papafotiou, G., Katrakili, N., and Talianidis, I. (2000) Transcriptional activation by hepatocyte nuclear factor-1 requires synergism between multiple coactivator proteins. *J. Biol. Chem.* **275,** 12515–12520
53. Cheriyath, V., Desgranges, Z. P., and Roy, A. L. (2002) c-Src-dependent transcriptional activation of TFII-I. *J. Biol. Chem.* **277,** 22798–22805
54. Inamoto, S., Segil, N., Pan, Z.-Q., Kimura, M., and Roeder, R. G. (1997) The cyclin-dependent kinase-activating kinase (CAK) assembly factor MAT1, targets and enhances CAK activity on the POU domains of octamer transcription factors. *J. Biol. Chem.* **272,** 29852–29858
55. Babu, M., Vlasblom, J., Pu, S., Guo, X., Graham, C., Bean, B. D., Burston, H. E., Vizeacoumar, F. J., Snider, J., Phanse, S., Fong, V., Tam, Y. Y., Davey, M., Hnatshak, O., Bajaj, N., Chandran, S., Punna, T., Christopolous, C., Wong, V., Yu, A., Zhong, G., Li, J., Stagljar, I., Conibear, E., Wodak, S. J., Emili, A., and Greenblatt, J. F. (2012) Interaction landscape of membrane-protein complexes in Saccharomyces cerevisiae. *Nature* **489,** 585–589
56. Bustamante, C., Liphardt, J., and Ritort, F. (2005) The nonequilibrium thermodynamics of small systems. *Phys. Today* **58,** 43–48
57. Seksek, O., and Bolard, J. (1996) Nuclear pH gradient in mammalian cells revealed by laser microspectrofluorimetry. J Cell Sci. **109,** 257–262
58. Th Brogt, M., and Planta, R. J. (1972) Characteristics of DNA-dependent RNA polymerase activity from isolated yeast nuclei. *Lett. FEBS* **20,** 47–52
59. Hancock, J. F., Paterson, H., and Marshall, C. J. (1990) A polybasic domain or palmitoylation is required in addition to the CAAX motif to localize p21ras to the plasma membrane. *Cell* **63,** 133–139
60. Trigg, S. A., Garza, R. M., MacWilliams, A., Nery, J. R., Bartlett, A., Castanon, R., Goubil, A., Feeney, J., O'Malley, R., Huang, S. C., Zhang, Z. Z., Galli, M., and Ecker, J. R. (2017) CrY2H-seq: a massively multiplexed assay for deep-coverage interactome mapping. *Nat. Methods* **14,** 819–825
61. Chen, J., Carter, M. B., Edwards, B. S., Cai, H., Sklar, L. A. (2012) High throughput flow cytometry based yeast two-hybrid array approach for large-scale analysis of protein-protein interactions. *Cytometry A* **81,** 90–98
62. Bolognesi, B., and Lehner, B. (2018) Reaching the limit. *eLife* **7**
63. Kolonin, M. G. Zhong, J. and Finley, R. L. (2000) Interaction mating methods in two-hybrid systems. Methods Enzymol. **328,** 26–46